Polymer Chemistry

Accepted Manuscript

This is an *Accepted Manuscript*, which has been through the Royal Society of Chemistry peer review process and has been accepted for publication.

Accepted Manuscripts are published online shortly after acceptance, before technical editing, formatting and proof reading. Using this free service, authors can make their results available to the community, in citable form, before we publish the edited article. We will replace this *Accepted Manuscript* with the edited and formatted *Advance Article* as soon as it is available.

You can find more information about *Accepted Manuscripts* in the Information for Authors.

Please note that technical editing may introduce minor changes to the text and/or graphics, which may alter content. The journal's standard Terms & Conditions and the Ethical guidelines still apply. In no event shall the Royal Society of Chemistry be held responsible for any errors or omissions in this *Accepted Manuscript* or any consequences arising from the use of any information it contains.

ROYAL SOCIETY OF CHEMISTRY

www.rsc.org/polymers

Polymer Chemistry

Article

Efficient red emission from poly(vinyl butyral) films doped with a novel europium complex based terpyridyl as ancillary ligand: synthesis, structural elucidation by Sparkle/RM1 calculation, and photophysical properties

Received 00th January 20xx,
Accepted 00th January 20xx

DOI: 10.1039/x0xx00000x

www.rsc.org/

Chaolong Yang, *[ab] Shaojun Liu,[a] Jing Xu,[bc] Youbing Li,[a] Mingyong Shang,[a] Lei Lei,[a] Guoxia Wang,[a] Jian He,[a] Xuanlun Wang,[a] Mangeng Lu[b]

A novel efficient antenna Eu-complex $Eu(TTA)_2Tpy\text{-}OCH_3.2H_2O$ based on the terpyridyl derivative 4'-(4-methoxyphenyl)-2,2':6',2''-terpyridine(Tpy-OCH_3) as ancillary ligand has been synthesized, structurally characterized, and its photophysical properties examined. The new Eu-complex displays bright red luminescence upon irradiation at the ligand-centered band in the range of 200–450 nm, irrespective of the medium. Sparkle/RM1 calculation was utilized for predicting the ground-state geometries of this complex. Theoretical Judd-Ofelt and photoluminescence parameters, including quantum efficiency, predicted from this model are in good agreement with the experimental values, proving the efficiency of this theoretical approach implemented in the LUMPAC software (http://lumpac.pro.br). The kinetic scheme for modeling energy transfer processes show that the main donor state is the ligand triplet state and that energy transfer occurs on both the $^5D_1$ (20.7%) and $^5D_0$ (79.3 %) levels. As an integral part of this work, the synthesis, characterization, and luminescent properties of poly(vinyl butyral) (PVB) polymer films doped with Eu-complex are also reported. Upon Eu-complexe $Eu(TTA)_2Tpy\text{-}OCH_3.2H_2O$ was doped into the PVB matrix forming the films, the PVB polymer matrix acting as a co-sensitizer for Eu^{3+} ion enhances the luminescent lifetimes and quantum efficiencies in comparison with the precursor complex. The new luminescent Eu/PVB films therefore show considerable promise for polymer light-emitting diode and active polymer optical fiber applications. To the best of our knowledge, this is the first report which detailed study the photophysical properties of doped europium fluorescent films based on PVB as the polymer matrix.

1 Introduction

Due to these unique optical properties, such as large antenna-generated shifts [1], monochromaticity, high luminescence efficiency, and long excited-state lifetimes, make europium complexes have significant technological applications in amplifiers for optical communications, optoelectronic, supra-molecular, luminescent probes for biological systems and sensors uses [2]. Unfortunately, the long luminescent lifetimes of europium ion result in a low absorption coefficient. To overcome the problem, organic ligands which have much large absorption coefficient are usually coordinated to sensitize europium complexes. So the design and synthesis of organic ligands with larger absorption coefficient are very important to improve luminescent properties of europium complexes.

As well-known, the β-diketone ligand class is emerging as one of the important "antennas" in terms of high harvest emissions because of the effectiveness of the energy transfer from this ligand type to the Eu^{3+} ion [3]. In general, β-diketonate europium complexes are isolated with two solvent molecules which quench the lanthanide emission by activation of non-radiative decay pathways [4]. To overcome this problem, the solvent molecules should be replaced by ancillary ligands containing chromophores that are equipped to play the antenna role [5]. Therefore, the positive effect of ancillary ligands like tpy (terpyridine) was often employed to replace the solvent molecules to enhance the luminescent intensity. Some reports have confirmed that tpy is an excellent neutral ligand for Eu-complexes; it can reduce the non-radiative decay of the excited states of the europium ion, improve the stability of the europium complexes, and increase the energy transfer efficiency from the ligands to the Eu^{3+}ions [6].

In the field of coordination compounds, the semiempirical Sparkle/RM1 model has proven to be effective in lanthanide chemistry because it allows the prediction of the coordination geometry for both small lanthanide complexes and more sophisticated structures in a relatively short time and with a low computational demand[7, 8]. Recent results have shown good prediction for the ground state geometry, when compared to single crystal data [9]. So, when the data of monocrystals for lanthanide complexes can not be obtained, the semiempirical Sparkle/RM1

[a] School of Materials Science and Engineering, Chongqing University of Technology, Chongqing 400054, PR China
[b] Key Laboratory of Polymer Materials for Electronics, Guangzhou Institute of Chemistry, Chinese Academy of Sciences, Guangzhou 510650, PR China
[c] Department of Chemistry, Graduate School of Science, Tohoku University, Aramaki -Azaaoba 6-3, Aoba-ku, Sendai, Japan
*Corresponding author E-mail: yclzjun@163.com; yclly2013@cqut.edu.cn (CL Yang)

model was often used to calculate the ground-state geometries of these lanthanide complexes.

As well-known, the lanthanide complexes typically display low thermal-stability, and limited photostability [10]. It is known that polymers provide a series of advantages for the development of molecular materials, for instance, thermal and chemical stability, flexibility, versatility, biocompatibility, hydrophobic-hydrophilic balance and the characteristic luminescence of lanthanide ions [11]. All of these features offer excellent expectation for fabricating a new class of highly luminescent materials [12]. A popular polymer matrix for use as a host for luminescent lanthanide complexes is poly(vinyl butyral) (PVB) which is a low-cost, good transparence and simply prepared polymer of excellent optical quality [13]. When lanthanide complexes incorporate with it forming a new complex-containing polymer/film, it will lead to significant flexibility, versatility, thermal and photo-stability [14]. Meanwhile, as is well-known, there are some carbonyl groups in PVB chain, but so far, the report about whether these carbonyl groups play a key role for improving luminescent properties of Eu-complex doped in PVB matrix is quite limited.

Therefore, in this work, to understand the role of PVB matrix in Eu-complex doped in PVB, we designed and synthesised a new and unsaturated europium complex based on terpyridyl(Tpy-OCH_3) as ancillary ligand, $Eu(TTA)_2$Tpy-$OCH_3.2H_2O$, calculate the ground state geometry using the Sparkle/RM1, and calculate the intensity parameters, transfer and back transfer rates and energy level populations. With these data we can compare the theoretical results to experimental ones and use the theoretical data to explain some experimentally observed facts. Further, in order to study the role of PVB matrix in doped films, this unsaturated europium complex was doped into the PVB matrix forming films, FTIR and PL results indicated carbonyl groups in PVB successfully replaced the water molecules and coordinated with Eu^{3+}. The overall aim of this work was to develop a simple and feasible method for the production of a luminescent material with the objective of obtaining information about the photo-luminescence (PL) behavior of the optical material incorporated into the PVB matrix. The sensitization effect of the polymer matrixes on the Eu^{3+} luminescent center is discussed in detail based on excitation and emission spectra, experimental intensity parameters, and quantum efficiency. To the best of our knowledge, this is the first report which detailed study the photophysical properties of doped europium fluorescent films based on PVB as the polymer matrix.

2 Experimental sections

2.1 Materials and instrument

Polyvinyl butyral (PVB) (AR, Mn = 98,400, polydispersity index (PDI) = 1.34, the butyral content 45.0-49.0% (wt%), water content less than 0.2 wt %), purchased from Sinopharm Chemical Reagent, China. Eu_2O_3 (99.99%) was purchased from a Chinese company, Beijing Founder. $EuCl_3.6H_2O$ was obtained by dissolving Eu_2O_3 in concentrated chlorhydric acid. 2-Thenoyltrifluoroacetone(TTA) was purchased from Aladdin Company, China, and other chemicals were all commercially available and used without further purification. FT-IR spectra were carried out using a Nicolet Is-10 (Nicolet) Fourier Transform Infrared Spectrometer. Elemental analysis data were obtained from Vario EL elemental analyzer. Differential scanning calorimetry (DSC) made on TA Q20 at a heating rate of 15°C/min under nitrogen. Thermogravimetric analysis was made with TA Q50 at a heating rate of 15°C/min under N_2 atmosphere and over a temperature range from 35 to 650 °C. All the ESI-MS spectra were recorded in LCQ DECA XP mass spectrometer. Elemental analysis data were obtained from Vario EL elemental analyzer. X-ray diffraction (XRD) patterns were determined with a DX-2500 diffractometer (Fangyuan, Dandong) using Cu Kα radiation (30 kV and 200 mA) at a step width of 0.04°. NMR spectra were taken on a DRX-400 MHz (Bruker) superconducting-magnet NMR spectrometer with TMS as an internal standard. UV-vis absorption spectrum was determined on a Shimadz spectrophotometer (UV 2540). The photoluminescence (PL) measurements in solid state and THF solution were conducted in a Hitachi F-4600 florescence spectrophotometer. Fluorescent lifetimes were obtained with the FLS920 steady state spectrometer with a pulsed xenon lamp.

2.2 Synthesis of 4'-(4-methoxyphenyl)-2,2':6',2''-terpyridine(Tpy-OCH_3)

2-Acetylpyridine (1.21 g, 10 mmol) was added into a solution of *p*-methoxybenzaldehyde (0.68 g, 5 mmol) in EtOH (50 mL). KOH pellets (0.78 g, 85%, 10 mmol) and ammonia solution (15 mL, 29.3%, 12 mmol) was then added to the solution. The solution was stirred at room temperature for 12 h. The milk-white solid was collected by filtration and washed with EtOH (3×20 mL). Yield: 1.1 g (65%). ^{1}H NMR (400 MHz $CDCl_3$): 8.64–8.72 (m, 6H, tpy), 7.84–7.88 (t, 4H, ArH), 7.32–7.35 (t, 2H, tpy), 7.0–7.02 (d, 2H, ArH), 3.87 (s, 3H, –OCH_3). ^{13}C NMR (100 MHz $CDCl_3$): 160.48,155.91, 149.29, 136.88, 130.59, 128.43, 123.74, 121.29, 118.23, 114.13, 55.31. ESI-MS: m/z 340.3 $(M + H)^+$. FT-IR (KBr pellet, cm^{-1}): 1602, 1585, 1568, 1521, 1468, 1392, 1265, 1190, 1042, 833, 793, 730, 662, 569, 517.

2.3 Synthesis of Eu-complex $Eu(TTA)_2$Tpy-$OCH_3.2H_2O$

The complex was prepared according to the well-established method [15]. Tpy-OCH_3 (0.39 g, 1 mmol) was dissolved in THF (50 mL), to which $Eu(TTA)_2.4H_2O$ (0.67 g, 1 mmol) was added. The whole mixture was refluxed for 3 h and cooled to room temperature. The resulting precipitate was collected and washed twice with water to give the target complex (0.79 g, 81%) as a light-yellow powder. ^{1}H NMR (400 MHz $CDCl_3$): 14.08 (s, 1H, tpy-H), 11.46 (s, 1H, tpy-H), 8.70 (d, 4H, tpy-H), 7.88 (s, 4H, tpy-H), 7.38 (s, 2H, tpy-H), 7.06 (d, 2H, ph-H),6.24 (d, 2H, Th-H), 5.38 (s, 2H, Th-H),4.47(s, 2H, Th-H), 3.88 (s, 3H, –OCH_3), 3.65(s, 2H, TTA-CH), 1.24(s, 4H, H_2O). (Found: C, 50.01; H, 3.01; N, 4.26. $EuC_{39}H_{29}F_6N_3O_5S_2$ [$Eu(TTA)_2$Tpy-OCH_3] requires C, 49.32; H, 3.08; N,4.42%). ESI-MS m/z: $[M+6H^++Na^+]^+$: 998.29. FT-IR (KBr pellet, cm^{-1}): 1605(C=O

stretching in TTA), 1540 (C=C stretching in TTA), 1312, 1187, 1137, 638(O→Eu), 456(N→Eu).

2.4 Synthesis of Eu-Complex-Doped PVB Polymer Films.

The PVB polymer was doped with the Eu-complex $Eu(TTA)_2Tpy\text{-}OCH_3.2H_2O$ in the proportions 1, 3, 5, and 7%(w/w). The PVB powder was dissolved in chloroform, followed by addition of the required amount of Eu-complex $Eu(TTA)_2Tpy\text{-}OCH_3.2H_2O$ in THF solution, and the resulting mixture was heated at 60 °C for 30 min. The polymer film was obtained after evaporation of excess solvent at 60°C.

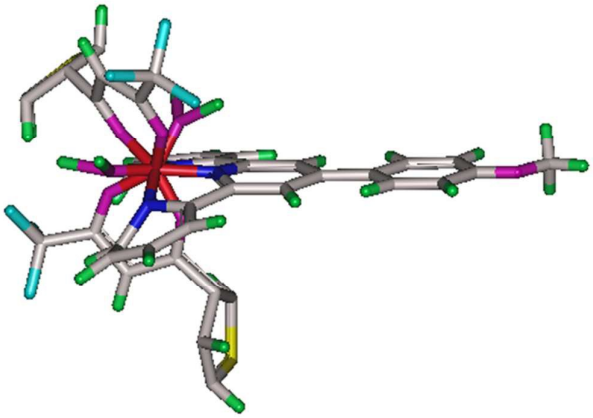

Figure 1 Ground-state geometry of $Eu(TTA)_2Tpy\text{-}OCH_3.2H_2O$ calculated using the Sparkle/RM1 model.

Table 1 Spherical atomic coordinates calculated via Sparkle/RM1 coordination polyhedron of the complex Eu $(TTA)_2Tpy\text{-}OCH_3.2H_2O$

	R (Å)	ϑ (degree)	φ (degree)
Eu^{3+}	0.000	0.000	0.000
N(Tpy-OCH_3)	2.531	136.635	89.449
N(Tpy-OCH_3)	2.547	76.451	65.365
N(Tpy-OCH_3)	2.548	147.71	28.492
O(TTA)	2.452	64.263	351.169
O(TTA)	2.448	122.125	330.532
O(TTA)	2.452	19.033	343.775
O(TTA)	2.454	73.603	31.062
O(H_2O)	2.527	79.169	277.297
O(H_2O)	2.532	83.799	325.025

3 Results and discussion

3.1 Geometry optimization, and simulation of UV and IR spectra for $Eu(TTA)_2Tpy\text{-}OCH_3.2H_2O$

In the field of coordination compounds, the semiempirical Sparkle model has proven to be effective in lanthanide chemistry because it allows the prediction of the coordination geometry for both small lanthanide complexes and more sophisticated structures in a relatively short time and with a low computational demand [16]. The optimized molecular structure of $Eu(TTA)_2Tpy\text{-}OCH_3.2H_2O$ predicted by Sparkle/RM1 model are displayed in **Figure 1**. Here, The Eu^{3+} ion in this compound is nine-coordinate and the coordination polyhedron can be approximately described as a tricapped trigonal prism, and the europium complex belongs to the C_1 point-group. The spherical atomic coordinates calculated *via* Sparkle/RM1 coordination polyhedron of this Eu-complex is summarized in **Table 1**. From the results we know that the central Eu^{3+} ion is coordinated with six oxygen atoms and three nitrogen atoms, four oxygen atoms are from the two β-diketonate ligands TTA, the other two oxygen atoms from the water molecules, and the three nitrogen atoms are from the ancillary ligand Tpy-OCH_3.The average bond length between the Eu^{3+} ion and the TTA oxygen atoms is 2.451Å, which is shorter than that of Eu^{3+} ion and water oxygen atoms (2.529 Å). This observation could be attributed to the presence of a formal negative charge on the TTA oxygen atoms which could enhance the binding to the Eu^{3+} cation due to electrostatic effects. The average bond length of Eu^{3+} ion and Tpy-OCH_3 nitrogen atoms is 2.542 Å. These average bond lengths are close to the distance estimated using X-ray diffraction data for the corresponding single crystal Eu-complex based on TTA and terpyridyl derivatives [17].

The experimental and simulated IR spectra of the Eu-complex $Eu(TTA)_2Tpy\text{-}OCH_3.2H_2O$ are shown in **Figure S1**. The calculation was made for a free molecule in vacuum, while the experiment was performed for the solid state and existed many interaction between molecules; furthermore, the anharmonicity in the real system was neglected for the vibration calculations. Therefore, they are disagreements between the calculated and experimental vibrational wavenumbers. Nevertheless, the characteristic stretching peaks of $Eu(TTA)_2Tpy\text{-}OCH_3.2H_2O$ can be realized, these absorbance peaks located at 1653, 1594 and 1485 cm^{-1} are attributed to the C=O and C=C stretching vibrations of the coordinated TTA ligand and C=N of the coordinated Tpy-OCH_3 ligand in the Eu-complex, respectively. A comparison of the calculated and experimental UV spectra for $Eu(TTA)_2Tpy\text{-}OCH_3.2H_2O$ is presented in **Figure S2**. As can be seen, the agreement between the simulated and experimental spectra is good. Whether in the calculated or in the experimental spectrum, two main absorption bands of the Eu-complex are easily observed, which are attributed to the singlet–singlet π→π enol absorption of TTA and Tpy-OCH_3 moieties in the Eu-complex. It is noteworthy that the obvious blue shift of these two absorption peaks in the calculated spectrum can be observed (the first and last absorption peak from 296 nm shift to 272 nm, and from 342 nm shift to 308 nm, respectively), which might be attributed to the solvent effects neglected in the calculation or any errors inherent in the method itself.

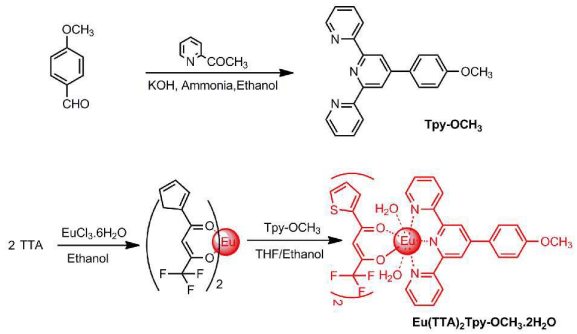

Scheme 1 Synthetic procedures of the Eu-complex $Eu(TTA)_2Tpy\text{-}OCH_3.2H_2O$.

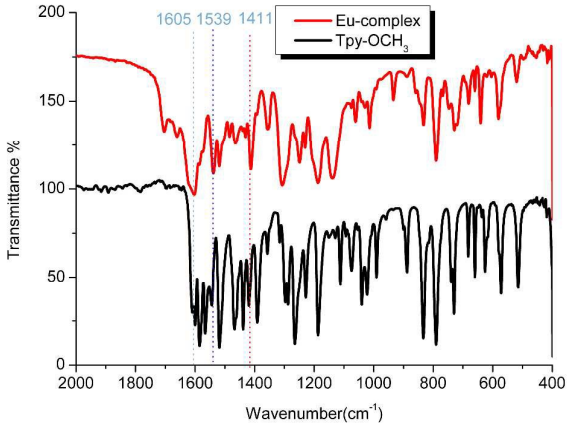

Figure 2 The FTIR spectra of ancillary ligand $Tpy\text{-}OCH_3$ and Eu-complex $Eu(TTA)_2Tpy\text{-}OCH_3.2H_2O$.

3.2 Design, Synthesis, and Characterization of ligand, Eu-complex and PVB fluorescent films

With the aim of studying the role of carbonyl groups in PVB chain in doped Eu-complex/PVB films, a novel ancillary ligand 4'-(4-methoxyphenyl)-2,2':6',2''-terpyridine ($Tpy\text{-}OCH_3$) and a corresponding unsaturated Eu-complex based $Tpy\text{-}OCH_3$ as ancillary ligand have been designed and synthesized. The ancillary ligand $Tpy\text{-}OCH_3$ was synthesized in 65% yield from the condensation of 2-acetylpyridine and *p*-methoxybenzaldehyde. The overall procedure is summarized in **Scheme 1**. The ligand was characterized by ^1H NMR and ^{13}C NMR(Supporting Information, **Figure S3 and S4**), FT-IR, and mass spectroscopic (ESI-MS) methods. The Eu-complex $Eu(TTA)_2Tpy\text{-}OCH_3.2H_2O$ was synthesized according to the well-established procedure with a high yield of 81%. The Eu-complex was characterized by FT-IR, ^1H NMR (**Figure S5**) and ESI-MS (**Figure S6**), and elemental analyses. The elemental analyses and ESI-MS studies revealed that the central Eu^{3+} ion is coordinated to an ancillary ligand $Tpy\text{-}OCH_3$, two TTA ligands, as well as two water molecules. Compared with the ligand $Tpy\text{-}OCH_3$, in the FT-IR spectrum of Eu-complex $Eu(TTA)_2Tpy\text{-}OCH_3.2H_2O$, three new absorbance peaks were observed at 1605, 1539 and 1411 cm^{-1} (**Figure 2**). They are attributed to the C=O and C=C stretching vibrations of the coordinated TTA ligand and the C=N stretching vibration of the coordinated $Tpy\text{-}OCH_3$ ligand in the Eu-complex, respectively. These results indicate that the ancillary ligand $Tpy\text{-}OCH_3$ and the first ligand TTA had successfully coordinated with the Eu^{3+} ion emission center.

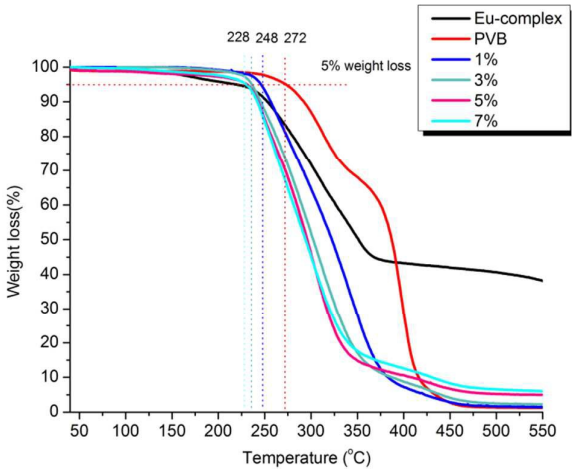

Figure 3 TGA curves of Eu-complex, PVB, and Eu/PVB films.

The thermal behavior of the Eu-complex $Eu(TTA)_2Tpy\text{-}OCH_3.2H_2O$ under a nitrogen atmosphere were examined by means of thermogravimetric analysis (TGA). The general profile of the weight loss for Eu-complex is displayed in **Figure 3**. It is clear from the TGA data that Eu-complex undergoes a mass loss of approximately 5.1% (Calcd: 3.8%) in the first step (103 to 228°C), which corresponds to the elimination of the coordinated water and solvent molecules. The second decomposition stage occurs from 229 to 373°C, and the mass loss is about 48.1% (Calcd. 43.7), which corresponds to the degradation of first ligand TTA. The last decomposition stage occurs from 376 to 690°C, which corresponds to the decomposition of ancillary ligand $Tpy\text{-}OCH_3$. The final residue is approximately 26% of the initial mass, it correspond to formation of the non-volatile europium (III) oxyfluoride.

The PVB matrix was doped with $Eu(TTA)_2Tpy\text{-}OCH_3.2H_2O$ in the proportions of 1, 3, 5, and 7% (w/w) and characterized by FT-IR spectroscopy. Compared with pure PVB matrix, a new absorption peak is found at 1605 cm^{-1} in the FT-IR spectroscopy of Eu/PVB films (**Figure 4**), the results indicates that the Eu-complex $Eu(TTA)_2Tpy\text{-}OCH_3.2H_2O$ successfully doped into the PVB matrix. The band at 1678 cm^{-1} for PVB corresponds to the C=O vibration, whereas for the Eu/PVB films, this vibration shifts to 1667 cm^{-1}. In turn, this implies that the Eu^{3+} complex is stabilized by means of interactions with the oxygen atoms of the carbonyl group of PVB.

The room-temperature X-ray diffraction patterns from 5 to 40° of complex $Eu(TTA)_2Tpy\text{-}OCH_3.2H_2O$ and Eu/PVB films are shown in **Figure S7**. It can be seen from the XRD results that the structural characteristics of the complex are different when the Eu-complex is incorporated into the PVB matrix, due to interactions between the

PVB and the Eu-complex. Two sharp crystal peaks centred about 30.72 and 31.54° are observed in XRD pattern of Eu-complex; however, there are no any crystalline regions in the XRD patterns of Eu/PVB films, the result indicates that Eu-complex can disperse in PVB matrix very well, and no molecular aggregation occurs in this system. This phenomenon can be attributed to the forming of cross-linked structure between carbonyl groups of PVB matrix and Eu3+, means every Eu-complex molecule was surrounded by different PVB chains in Eu/PVB films. **Figure 5** illustrates in a schematic way how the europium complex is coordinated to the PVB backbone. Such interactions might stem from the donation of a pair of electrons from the carbonyl oxygen to the lanthanide ions [18].

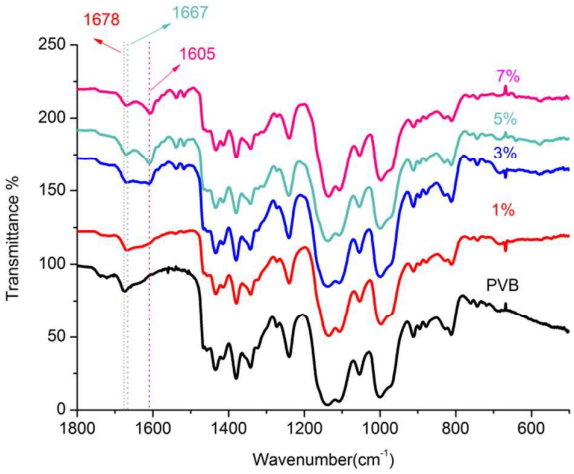

Figure 4 The FTIR spectra of PVB and Eu/PVB films.

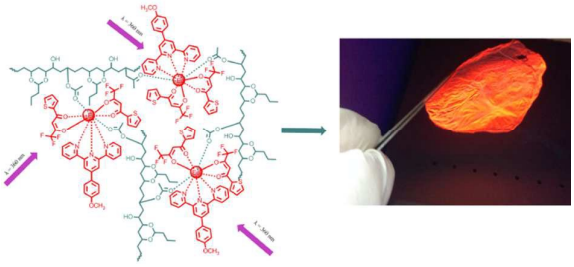

Figure 5 A schematic illustration of the structure of $Eu(TTA)_2Tpy\text{-}OCH_3.2H_2O$ complex doped in PVB matrix.

The thermal stability of the Eu-complex is very important because decomposition leads to decreased fluorescent performance. The differential scanning calorimetry (DSC) analysis of the PVB matrix and Eu/PVB films were measured to investigate their phase stability (**Figure S8**). The glass transition temperature (T_g) of Eu/PVB film which doped 1% Eu-complex is 74.58 °C, which is lower than that of the pure PVB(T_g 78.07 °C). It is noted that the T_g values of doped 3%, 5% and 7% are reduced to 73.75, 73.02, and 71.83 C, respectively, which means that the rigidity of the Eu/PVB films was reduced with increasing Eu-complex content.

The thermal stability of Eu/PVB films was investigated by thermogravimetric analysis (TGA) (**Figure 3**). The temperatures of the thermal decomposition (T_d, 5% weight loss temperature) of Eu/PVB films doped with the Eu-complex at a ratio of 1, 3, 5, and 7(w/w) are 248, 236, 231 and 228 °C, respectively, which are lower than that of undoped PVB film (272 °C). Nevertheless, these Eu/PVB films still have good thermal stability with 5% weight loss occurring at greater than 220 °C, and still can satisfy application in many fields.

As can be seen, the TG curves recorded in the temperature interval from 30 to 210 °C exhibited almost no mass loss event (near 0.26% mass loss can be attributed to the moisture in environment and technical errors). This reveals that the water molecules coordinated to the Eu^{3+} ion of the dihydrate complex precursor are absent after the doping reaction process. When the $Eu(TTA)_2Tpy\text{-}OCH_3.2H_2O$ complex is embedded into the PVB matrix, the coordination of the two water molecules is replaced by the interaction between the Eu^{3+} complex and the oxygen atoms of the PVB matrix (**Figure 5**), in agreement with the results of other polymer systems previously analyzed [19].

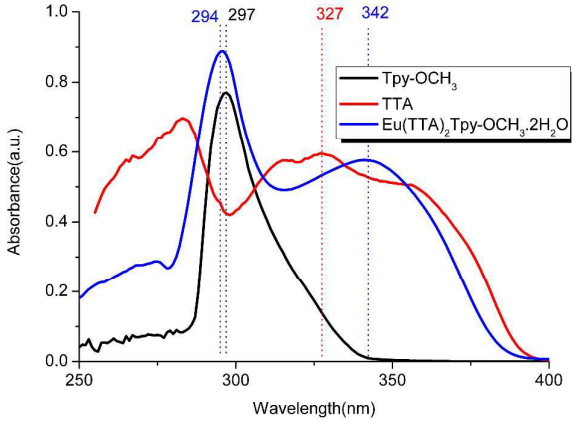

Figure 6 UV-vis spectra of TTA, ancillary ligand $Tpy\text{-}OCH_3$, and Eu-complex $Eu(TTA)_2Tpy\text{-}OCH_3.2H_2O$ in THF solution(1×10^5 mol/L).

3.3 Electronic Absorption Spectroscopy

The UV-vis absorption spectra for free ligands $Tpy\text{-}OCH_3$, TTA and Eu-complex $Eu(TTA)_2Tpy\text{-}OCH_3.2H_2O$ in THF solution (1×10^5 mol/L) are shown in **Figure 6**. The trend in the absorption spectra of Eu-complex is identical to the ones observed for the free ligands, indicating that the singlet excited states of the ligands are not significantly affected by the complexation to the Eu^{3+} ion. Two main absorption bands of the $Eu(TTA)_2Tpy\text{-}OCH_3.2H_2O$ are easily observed, at 294 nm and 342 nm, which are attributed to the singlet–singlet π→π enol absorption of TTA and $Tpy\text{-}OCH_3$ moieties in the Eu-complex. However, compared with the ancillary ligand $Tpy\text{-}OCH_3$, a small blue shift is observed in the absorption maximum of Eu-complex (from 297 nm shift to 294 nm), and it is attributable to the ring-forming by Eu^{3+} coordination. In addition, due to the formation of larger conjugated chelate rings in Eu-complex, the

located 327 nm absorption bands for free ligand TTA shifts to 342 nm for Eu-complex. The presence of the ancillary ligand Tpy-OCH_3 not only enhances the absorption intensity but also satisfies the high coordination number of the central Eu^{3+} ion and thus improves the coordination and thermal stabilities of Eu-complex. The molar absorption coefficient values for $Eu(TTA)_2$Tpy-$OCH_3.2H_2O$ at 294 nm are 7.13×10^4 L mol^{-1} cm^{-1}, which is higher than that for ligand Tpy-OCH_3 at 297 nm (5.14 × 10 4 L mol^{-1} cm^{-1}). The magnitude of the value is approximately 1.38 times higher than that for the ligand, and this trend is accordant to the presence of one ancillary ligand Tpy-OCH_3 in Eu-complex. Note also that the large molar absorption coefficient obtained for the newly designed Tpy-OCH_3 ligand indicates that it has a strong ability to absorb light.

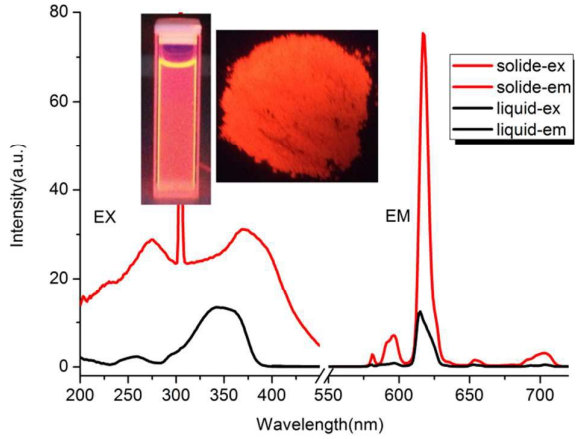

Figure 7 The PL spectra of Eu-complex $Eu(TTA)_2$Tpy-$OCH_3.2H_2O$ in solid and in THF solution(1×10^4 mol/L). Left: excitation spectra (λ_{em} = 615 nm), right: emission spectra (λ_{ex} = 365 nm).

3.4 Luminescence properties of Eu-complex

Excitation spectra of the Eu-complex recorded at room temperature in solid state and in THF solution by monitoring the Eu($^5D_0 \rightarrow {}^7F_2$) transition at 613 nm are depicted in **Figure 7**. For solution excitation spectra, there was one intense broad band at 278-395 nm. While in solid state excitation spectra, it can be seen clearly that intense broad band between 200 nm and 450 nm dominate the large portions of excitation spectra of Eu-complex, which were attributed to the π→π* transitions of ligands (Tpy-OCH_3 and TTA) from the comparison of the UV-vis spectra in **Figure 6**. In comparison with the excitation broad bands of ligands, the direct excitation peaks of europium ion were much weaker. This suggested that emission of europium by ligands were much more efficient than direct excitation of the europium complex. Meanwhile, the strongly bright red emission of Eu-complex $Eu(TTA)_2$Tpy-$OCH_3.2H_2O$ in solid and in THF solution, upon illuminating with a 365 nm excitation light provided by a 12w ultraviolet lamp, can be easily observed by the naked eye (Inset of **Figure 7**).

The mechanism of the energy transfer from ligands to metal ions had been widely discussed to interpret the luminescence of lanthanide compounds [20]. From the results discussed above, we can presume that the energy gaps of the Eu^{3+} ion were comparable with the triplet state energy of the ancillary ligand Tpy-OCH_3, and then efficient energy transfer can take place from Tpy-OCH_3 to europium ion, we will detailed discussed the energy transfer progress as below. The Eu-complex exhibited characteristic red emission of Eu^{3+} ion by 365 nm excitation and suggested the complex can be potential red fluorescent materials.

The emission spectra of $Eu(TTA)_2$Tpy-$OCH_3.2H_2O$ in solid state was shown in **Figure 7**, and characteristic Eu^{3+} ion emission was observed. The lines were distributed mainly in the 550-715 nm range, which were associated with the 4f → 4f transitions of the $^5D_0$ excited state to its low-lying ^7F_J(J = 0, 1, 2, 3 and 4) levels of Eu^{3+} ions. No emission peaks from the ligands were observed under this excitation, further confirming that the energy transfer from ligands to Eu^{3+} ion center was quite efficient in this Eu-complex. As well-known, the emissions of Eu^{3+} ion were usually employed as a sensitive probe to investigate the coordination and local environment around cations. For Eu^{3+} ion transitions, observed in the emission spectrum, occur via three main mechanisms: forced electric dipole, magnetic dipole, and dynamic coupling. From the emission spectra, we can see the emissions bands at about 581 nm and 654 nm were very weak since their corresponding transitions $^5D_0 \rightarrow {}^7F_{0,3}$ were forbidden both in magnetic and electric dipole schemes. A prominent feature that may be noted in these spectra was very high intensity of $^5D_0 \rightarrow {}^7F_2$ transition at 614 nm. It was well-known to us that the $^5D_0 \rightarrow {}^7F_1$ transition was a parity allowed magnetic dipole (MD) and is nonsensitive to the local structure environment, while the $^5D_0 \rightarrow {}^7F_2$ transition was a typical electric dipole (ED) transition and was sensitive to the coordination environment to the europium ion. When the interaction of the rare earth complex with its local environment was stronger, the complex became more nonsymmetrical, and the intensity of the electric-dipolar transitions became more intense. As a result, the integration intensity ratio of the $^5D_0 \rightarrow {}^7F_2$ transition to $^5D_0 \rightarrow {}^7F_1$ transition (I_2/I_1) had been widely used as an indicator of europium ion site symmetry. The calculated results were shown in **Table 2**.

Table 2 Experimental and calculated values of intensity parameters (Ω_2), Radiative (A_{rad}) and nonradiatve (A_{nrad}) rates, lifetime (τ), emission quantum efficiency (η) for complex $Eu(TTA)_2$Tpy-$OCH_3.2H_2O$

Structure	R_{02}	$\Omega_2(10^{-20}\,cm^2)$	$\Omega_4(10^{-20}\,cm^2)$	$\Omega_6(10^{-20}\,cm^2)$	A_{rad}/S^{-1}	τ/ms(solid/THF solution)	η(%)
Experimental data	0.043	15.12	2.84	--	544.70	0.57/0.36	31.05

Sparkle/RM1 Structure	--	15.12	2.84	0.51	549.41	--/--	31.32

Whether in solid state or in THF solution, the intensity ration of $Eu(TTA)_2Tpy\text{-}OCH_3.2H_2O$ was relatively high. The values of the intensity rations (I_2/I_1) for Eu-complex is 13.52 in THF solution and is 10.27 in solid state, respectively. Especially, the value in THF is higher than in solid state. Why? The result maybe induced by the solvent molecules replaced the water molecules in $Eu(TTA)_2Tpy\text{-}OCH_3.2H_2O$. This ratio was only possible when the Eu^{3+} ion did not occupy a site with inversion symmetry. It was clear that strong coordination interaction took place between the organic ligands and Eu^{3+} ion. Further, the emission spectra of the complex showed only one line for $^5D_0 \rightarrow {}^7F_0$ transition, indicating that the presence of a single chemical environment around the europium ions [21]. In addition, no emission from the ligands was observed in **Figure 7**, it indicated that a very efficient energy transfer occurred from the ligands to the central Eu^{3+} ion.

To better understand the luminescent properties of Eu-complex $Eu(TTA)_2Tpy\text{-}OCH_3.2H_2O$ in solid and THF solution, the room temperature (RT) luminescence decay curves of the $^5D_0$ excited state were measured by monitoring the most intense emission lines ($^5D_0 \rightarrow {}^7F_2$) of europium ion center at 614 nm, and under excitation 360 nm Xenon lamp. The RT lifetime values (τ) of the $^5D_0$ level were determined by fitting the luminescence decay profiles with monoexponential functions, irrespective of the media. This is consistent with a single major emitting species in this Eu-complex, which was in agreement with the results of only one $^5D_0 \rightarrow {}^7F_0$ line in the emission spectra and the calculated results of Sparkle/RM1. Lifetime values gathered in **Table 2** show a 37% reduction in going from solid state to the solution for this complex, from 0.57 ms to 0.36 ms.

The intrinsic luminescent quantum efficiency (η) of the $^5D_0$ emission level in this Eu-complex at room temperature was obtained based on the luminescence data. Eq. (1) a means to determine the η values from experimental spectroscopic data [22].

$$\eta = \frac{A_{rad}}{A_{rad} + A_{nrad}} \qquad (1)$$

Where, A_{rad} and A_{nrad} are radiative and nonradiative transition rates, respectively. The denominator in Eq. (1) is calculated from the lifetime of the emitting level ($1/\tau = A_{rad} + A_{nrad}$). In the case of europium luminescence the value of A_{rad} can be estimated by spectral analysis with the help of Eq. (2) [23].

$$A_{rad} = \frac{A_{0-1} h\omega_{0-1}}{S_{0-1}} \sum_{J=0}^{4} \frac{S_{0-J}}{h\omega_{0-J}} \qquad (2)$$

Where, J represents the final $^7F_{0\text{-}6}$ levels, S is the integrated intensity of the particular emission lines and hw stands for the corresponding transition energies. $A_{0\text{-}1}$ is the Einstein coefficient of spontaneous emission between the $^5D_0$ and the $^7F_1$ Stark levels. The branching ratios for the $^5D_0 \rightarrow {}^7F_{5,6}$ transitions must be neglected as they are too weak to be observed experimentally. Therefore, their influence can be ignored in the depopulation of the $^5D_0$ excited state. The $^5D_0 \rightarrow {}^7F_1$ transition does not depend on the local ligand field seen by europium ions and, thus, may be used as a reference for the whole spectrum, in vacuo $A_{0\text{-}1}$ = 14.65 s^{-1} [24]. An average refractive index equal to 1.5 was considered, leading to $A_{0\text{-}1} \approx 50 s^{-1}$.

According to the above discussion, the intrinsic luminescence quantum efficiency of this Eu-complex in solid can be determined, as show in **Table 2**.

From the results of **Table 2**, the Eu-complex $Eu(TTA)_2Tpy\text{-}OCH_3.2H_2O$ exhibited relatively high luminescence quantum efficiency (31.05%), indicating that the energy transfer from ligands($Tpy\text{-}OCH_3$ and TTa) to emitted center Eu^{3+} ion was very efficient.

Judd–Ofelt theory is a useful tool for analyzing f-f electronic transitions [25]. Interaction parameters of ligand fields are given by the Judd–Ofelt parameters Ω_λ(where λ = 2, 4, and 6). In particular, Ω_2 is more sensitive to the symmetry and sequence of ligand fields. To produce faster Eu^{3+} radiation rates, antisymmetrical Eu^{3+} complexes with larger Ω_2 parameters need to be designed. The experimental intensity parameters (Ω_2 and Ω_4) for this Eu-complex $Eu(TTA)_2Tpy\text{-}OCH_3.2H_2O$ was determined from the emission spectra, based on the $^5D_0 \rightarrow {}^7F_2$ and $^5D_0 \rightarrow {}^7F_4$ electronic transitions of the Eu^{3+} ion, and they are estimated according to the following eq 3 [26]:

$$W_l = \frac{3hc^3 A_{0-l}}{4e^2 w^3 c \left\langle {}^5D_0 \left\| U^{\langle l \rangle} \right\| {}^7F_J \right\rangle^2} \qquad (3)$$

Where, e is the electronic charge. $\chi = n_0 (n_0^2 + 2)^2/9$ is a Lorenz local field correction. The square reduced matrix elements are $\langle {}^5D_0\ U^{(2)}\ F_2 \rangle^2 = 0.0032$ and $\langle {}^5D_0\ U^{(4)}\ F_4 \rangle^2 = 0.0023$, and an average index of refraction equal to 1.5 was used. The transition $^5D_0 \rightarrow {}^7F_6$ is not observed experimentally thus the experimentalΩ_6 parameter cannot be estimated.

Table 2 presents the experimental and theoretical values for the intensity parameters (Ω_2, Ω_4 and Ω_6). Firstly, we can note the good agreement between the theoretical and experimental values for Ω_2 and Ω_4 parameters. The Ω_6 parameter was only determined theoretically, since the $^5D_0 \rightarrow {}^7F_6$ transitions are not observed experimentally. The high values of Ω_2 might be interpreted as a consequence of the hypersensitive behavior of the $^5D_0 \rightarrow {}^7F_2$ transition, which suggests that the dynamic coupling mechanism is

quite operative and that the chemical environment is highly polarizable. The Ω_4 parameter is less sensitive to the coordination sphere than Ω_2; However, its value reflects the chemical environment rigidity surrounding the Eu^{3+} cation. The relatively low values of the Ω_4 parameter indicate rigidity associated with the coordinated sphere of the Eu-complex.

The theoretical radiative and nonradiative rates, and quantum efficiencies, are also in good agreement with the experimental values. The value of the emission quantum efficiency, in principle, should not be dependent on the T_1 position. Thus, the η behavior of Eu-complex will reflect vibronic couplings between the Eu^{3+} ion and the ligands, and it was influenced by the countercations.

In addition, **Table 2** presents also the R_{02} intensity parameter, which is the ratio between the intensities of the $^5D_0 \rightarrow {}^7F_0$ and $^5D_0 \rightarrow {}^7F_2$ transitions. The R_{02} parameter may give information on the *J*-mixing effect associated with the $^5D_0 \rightarrow {}^7F_0$ transition, as previously described. In this case, this effect is mainly due to the mixing between the $^7F_2$ manifold and the $^7F_0$ level though the rank-two components of the ligand field. The R_{02} value for this Eu-complex is relatively small (0.043), suggesting that the *J*-mixing effect is much smaller in this complex.

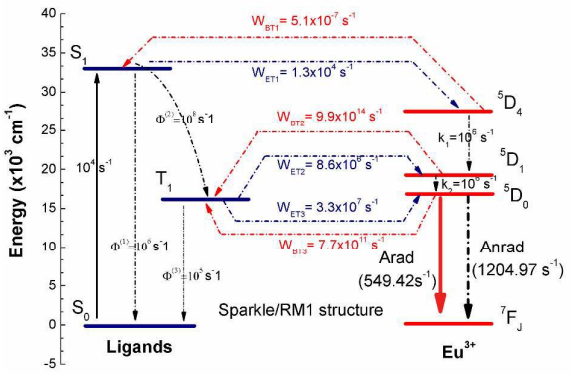

Figure 8 Schematic energy level diagram, energy transfer processes, and transfer rates for Eu-complex $Eu(TTA)_2Tpy\text{-}OCH_3.2H_2O$.

3.5 Modeling of the energy transfer progress

For the Eu-complex $Eu(TTA)_2Tpy\text{-}OCH_3.2H_2O$, the energies of the triplet and singlet states calculated for the Sparkle/RM1 structure using the INDO/S-CIS method are 15,208 cm^{-1} and 32,590 cm^{-1} , respectively. Modeling of the sensitization process of this Eu-complex was made according to **Figure 8**. The R_L parameter is the distance from the donor state located at the organic ligands and the Eu^{3+} ion nucleus. This quantity has been calculated by:

$$R_L = \frac{\sum_i c_i^2 R_{L,i}}{\sum_i c_i^2} \qquad (4)$$

with c_i being the molecular orbital coefficient of the atom i contributing to the ligand state (triplet or singlet) involved in the energy transfer, and $R_{L,i}$ corresponding to the distance from atom i to the Eu^{3+} ion. The two complexes show favorable R_L values for obtaining efficient energy transfer rates.

The potential receiving levels of Eu^{3+} ion, taking into account the selection rules and the $^7F_{0,1}$ population at room temperature, are $^5D_4$ (~27,500 cm^{-1}), $^5D_1$ (~19,000 cm^{-1}), and $^5D_0$ (~17,250 cm^{-1}). Intramolecular energy transfer, back-transfer rates, and the percentage contribution of each process to the overall energy transfer are presented in **Table 3** for this Eu-complex. The simulation points to a rather slow transfer from the singlet state onto Eu($^5D_4$), $>10^2$ slower than the transfer from the triplet state to either $^5D_1$ or $^5D_0$. However, regarding the latter, back transfer processes are much faster than for $^5D_4$; nevertheless, the S_1- to- $^5D_4$ pathway plays a negligible role(the percentage contribution is only 0.03%). Compared to $^5D_1$, the energy transfer rates of the transfer to $^5D_0$ is 2.8 times faster; in addition, back transfer from $^5D_1$ is much faster than from $^5D_0$, so that the T_1 -to- $^5D_0$ process accounts for slightly more than three fourths (79.3%) of the total energy transfer.

Table 3 Calculated values of excited state singlet and triplet energies, R_L values, intrenamolecular energy transfer (W_{ET}) and back transfer (W_{BT}) rates for complex $Eu(TTA)_2Tpy\text{-}OCH_3$

ligand state→4f state (cm^{-1})	R_L (Å) [a]	W_{ET} (s^{-1})	W_{BT} (s^{-1})	Contribution (%)
S_1 (32590) →$^5D_4$ (27586)	5.0665	1.3×10^4	5.1×10^{-7}	0.03
T_1 (15208) →$^5D_1$ (19027)	5.2520	8.6×10^6	9.9×10^{14}	20.7
T_1 (15208) →$^5D_0$ (17293)	5.2520	3.3×10^7	7.7×10^{11}	79.3

[a] The R_L value is the distance from the donor state located on the organic ligands and the Eu^{3+} ion nucleus.

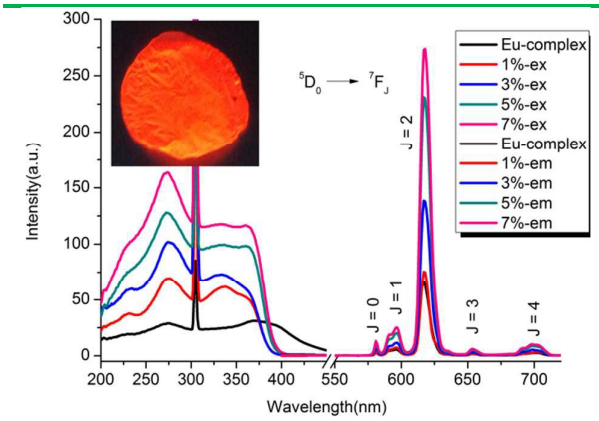

Figure 9 The PL spectra of Eu-complex and Eu/PVB films in solid. Left: excitation spectra (λ_{em} = 615 nm), right: emission spectra (λ_{ex} = 365 nm).

3.6 Photophysical Properties of Eu-Complex Doped in PVB matrix films

Lanthanide complexes incorporated into polymer matrixes represent a new class of materials that combine with the characteristics of both complexes and polymers, thus making them ideal candidates for use in wide range of new technologies [27]. In this manuscript, we describe the incorporation of a newly designed, highly luminescent complex into PVB, a well-known, low-cost, easily prepared polymer of excellent optical and mechanical quality. **Figure 9** shows the excitation spectra of the PVB matrix films doped with Eu-complex $Eu(TTA)_2Tpy\text{-}OCH_3.2H_2O$ at different concentrations 1, 3, 5 and 7% (w/w), and recorded at room temperature in the spectral range of 200 to 500 nm, by monitoring the emission at 613 nm. The spectral region from 200 to 400 nm is dominated by an intense broad band which is assigned to the polymer matrix and organic ligands absorption, and subsequent efficient intramolecular energy transfer to the Eu^{3+} ion. Furthermore, the typical intraconfigurational transitions are absent in these excitation spectra, owing to efficient energy transfer from the organic moiety to the Eu^{3+} ion. These facts suggest the PVB matrices serve as efficient co-sensitizers for the Eu^{3+} ion.

Table 4 Experimental Intensity parameters$\Omega_{2,4}$ and luminescent parameters for PVB films doped with various amounts of the complex $Eu(TTA)_2Tpy\text{-}OCH_3.2H_2O$, at 298 K

System	$\Omega_2(10^{-20}\,cm_2)$	$\Omega_4(10^{-20}\,cm_2)$	A_{rad}/S^{-1}	A_{nrad}/S^{-1}	τ/ms	η(%)	I_2/I_1	CIE(x, y)
$Eu(TTA)_2Tpy\text{-}OCH_3.2H_2O$	15.12	2.84	544.70	1209.69	0.57	31.05	10.27	0.67, 0.33
Eu-complex/PVB-1%	18.15	2.91	636.56	976.35	0.62	39.47	11.57	0.63, 0.31
Eu-complex/PVB-3%	18.78	2.95	656.06	814.53	0.68	44.61	11.92	0.66, 0.32
Eu-complex/PVB-5%	18.53	2.95	648.58	702.77	0.74	48.00	11.85	0.67, 0.33
Eu-complex/PVB-7%	17.41	2.77	612.39	537.04	0.87	53.28	11.18	0.67, 0.33

The emission spectra of PVB doped with Eu-complex at a variety of concentrations and excited at 365 nm exhibit five characteristic emission bands that are assigned to the $^5D_0 \rightarrow {}^7F_J$ (J = 0-4) transitions of the Eu^{3+} ion. As displayed in Figure 9, the luminescent intensity of the Eu^{3+} emission at 617 nm increases with increasing Eu^{3+} content, the phenomenon of concentration quenching does not occurred with the increasing Eu^{3+} content. The transition of highest intensity is dominated by the hypersensitive $^5D_0 \rightarrow {}^7F_2$ transition at approximately 617 nm, which implies that the Eu^{3+} ion does not occupy a site with inversion symmetry. Moreover, the presence of only one sharp peak in the region of the $^5D_0 \rightarrow {}^7F_0$ transition at 581 nm suggests the occurrence of a unique chemical environment around the Eu^{3+} ion of symmetry type C_s , C_n , or C_{nv}. It is well-known that the magnetic-dipole transition $^5D_0 \rightarrow {}^7F_1$ is nearly independent of the ligand field and therefore can be used as an internal standard to account for ligand differences. The electric-dipole transition $^5D_0 \rightarrow {}^7F_2$, the so-called hypersensitive transitions, is sensitive to the symmetry of the coordination sphere. The intensity ratio of the magnetic dipole transition to the electric dipole transition in the lanthanide complex measures the symmetry of the coordination sphere. The intensity ratios (I_2/I_1) of the $^5D_0 \rightarrow {}^7F_2$ transition to the $^5D_0 \rightarrow {}^7F_1$ transition in the Eu/PVB films were shown in **Table 4**. Compared with the undoped Eu-complex, the I_2/I_1 of Eu/PVB films is higher; these results suggest that, when the Eu-complex is incorporated into the microcavities of the PVB matrix, the Eu^{3+} ions exhibit different local environments because of the influence of the surrounding polymer. The symmetry of the coordination sphere for the Eu^{3+} ions changes moderately in the Eu/PVB films as compared to the undoped Eu-complex. When incorporated into the microcavities of the PVB matrix, however, the complexes exhibit disorder of a certain magnitude. Under the influences of the electric field of the surrounding ligands, the distortion of the symmetry around the Eu^{3+} ion by the capping PVB results in the polarization of the Eu^{3+}, which increases the probability for electric dipole, allowed transition. The influences of PVB on the coordinative environment of the Eu^{3+} ions changes the energy transfer probabilities of the electric dipole transitions, accounting for the increases in luminescent intensity of the 617 peak.

In addition, the Eu-complex and the all Eu/PVB films exhibit characteristic red emission of Eu^{3+} under UV 365 nm excitation, and it is suggested that these comlexes can be potential red fluorescent materials. The CIE chromaticity coordinates of Eu-compex, 1%, 3%, 5%, and 7% from the emission spectra are (0.67, 0.33), (0.63, 0.31), (0.66, 0.32), (0.67, 0.33) and (0.67, 0.33), respectively, which indicates pure red emission. The results are important because they indicate these materials can be used in some special fields such as OLEDs, optoelectric devices, etc.

The luminescence decay curves of Eu/PVB films were obtained by monitoring the emission at the hypersensitive $^5D_0 \rightarrow {}^7F_2$ transition

(613 nm) and excitation at the $^7F0 \rightarrow {}^5L$ transition (365nm). These data were adjusted with a first-order exponential decay function and the lifetime values (τ) of the emitter $^5D_0$ level of the doped systems were determined and are listed in **Table 4**. All τ values of doped polymer systems are higher than that of the Eu-complex indicating that radiative processes are operative in all the doped PVB films due to the absence of multiphonon relaxation by coupling with the OH oscillators from the $Eu(TTA)_2Tpy\text{-}OCH_3.2H_2O$.

The experimental intensity parameters (Ω_2 and Ω_4) for the doped Eu/PVB films and $Eu(TTA)_2Tpy\text{-}OCH_3.2H_2O$ complex are listed in **Table 4**. Large values of Ω_2 are observed and can be validated as a consequence of two concurrent factors. The first one is the symmetry around the Eu^{3+} ion, allowing the appearance of all odd-rank components in the noncentrosymmetric ligand field. The other factor is related to the hypersensitive character of the $^5D_0 \rightarrow {}^7F_2$ transition of the Eu^{3+} ion, suggesting that a dynamic coupling mechanism is operative and the chemical environment around the metal ion is highly polarizable. Especially, the values of Ω_2 of Eu/PVB films are higher the precursor $Eu(TTA)_2Tpy\text{-}OCH_3.2H_2O$, it was attributed to the –C=O groups successfully coordinated with the Eu^{3+} in Eu/PVB films, and effectively increased the asymmetry around the Eu^{3+}.

The radiative (A_{rad}) and non-radiative (A_{nrad}) decay rates, and quantum efficiencies (η) of the Eu/PVB films doped with $Eu(TTA)_2Tpy\text{-}OCH_3.2H_2O$ at different doping concentrations are presented in Table 4. Compared with the precursor $Eu(TTA)_2Tpy\text{-}OCH_3.2H_2O$, all the PVB doped films exhibit more excellent quantum efficiency values, ranging from 39.47 to 53.28%. These spectral data indicate that beyond immobilizing the Eu^{3+} ions among matrices, the PVB also acts as sensitizer of the system which greatly enhances the luminescence of the Eu^{3+} ion. It is well-known that the efficiency of the intermolecular energy transfer is strongly dependent on the distance between the donor and acceptor [28]. According to this point of view, it is suggested that for the present system, the PVB molecule, because of its long chain, has the capability to enwrap the $Eu(TTA)_2Tpy\text{-}OCH_3.2H_2O$ complex and keeps the acceptor and donor close. In such a case, energy can be transferred efficiently from ligand to Eu^{3+}, resulting in the enhancement of intrinsic Eu^{3+} emission of a $Eu(TTA)_2Tpy\text{-}OCH_3.2H_2O$. Thus the preserved rigidity in the complex structure in PVB could be the origin of the enhanced quantum efficiencies. To the best of our knowledge, this is the first report which detailed study the photophysical properties of doped europium fluorescent films based on PVB as the polymer matrix.

4 Conclusions

We have designed, synthesized, and characterized a novel nine-coordinate, highly luminescent europium complex based on terpyridyl derivative $Tpy\text{-}OCH_3$ as ancillary ligand. The structure of this Eu-complex is predicted for this chelate by Sparkle/RM1 calculations. The new complex displays efficient sensitized luminescence in solid with a quantum efficiency of 31.05%. Additionally, the newly designed europium complex was incorporated into PVB polymer films, which were shown to exhibit exceptionally high PL quantum efficiencies (39.47-53.28%). This implies that the PVB with high molecular weight enwraps the Eu-complex and keeps the donor and acceptor close, which results in the effective intermolecular energy transfer and, consequently, the high sensitization efficiency. In conclusion, the PVB films doped with the Eu-complex show promising PL efficiency and therefore have potential applications as polymer light-emitting diodes and active polymer optical fibers.

Acknowledgments

This work is financially supported by the National Natural Science Foundation of China (No. 21404017), and the Chongqing Science and Technology Innovation Capacity Building Project (Project No. cstc2013kjrc-qnrc50003).

Notes and references

1 P. A. Tanner. Chem. Soc. Rev. 2013, 42, 5090 – 5101.
2 (a) J.-C. G. Bünzli, Chem. Rev., 2010, 110, 2729; (b) C. Coluccini, P. Metrangolo, M. Parachini, D. Pasini, G. Resnati and P. Righetti, J. Polym. Sci., Part A: Polym. Chem., 2008, 46, 5202–5213; (c) J. Kido and Y. Okamoto, Chem. Rev., 2002, 102, 2357; (d) J. Wang, R. Wang, J. Yang, Z. Zheng, M. D. Carducci, T. Cayou, N. Peyghambarian and G. E. Jabbour, J. Am. Chem. Soc., 2001, 123, 6179; (e) M. Caricato, C. Coluccini, D. V. Griend, A. Forni and D. Pasini. New J. Chem., 2013,37, 2792-2799.; (f) D. Pasini, P. P. Righetti and V. Rossi, Org. Lett., 2002, 4, 23–26.
3 (a) Binnemans, K. Chem. Rev. 2009, 109, 4283 – 4374. (b) Ambili Raj,D. B.; Biju, S.; Reddy, M. L. P. Inorg. Chem. 2008, 47, 8091 – 8100. (c) Remya,P. N.; Biju, S.; Reddy, M. L. P.; Cowley, A. H.; Findlater, M. Inorg. Chem. 2008, 47, 7396 – 7404. (d) Biju, S.; Reddy, M. L. P.; Cowley, A. H.; Vasudevan, K. V. Cryst. Growth Des. 2009, 9, 3562 – 3569. (e) Biju, S.; Ambili Raj, D. B.; Reddy, M. L. P.; Jayasankar, C. K.; Cowley, A. H.; Findlater, M. J. Mater. Chem. 2009, 19, 1425 – 1432. (f) Ambili Raj, D. B.; Biju, S.; Reddy, M. L. P. Dalton Trans. 2009, 36, 7519 – 7528. (g) Ambili Raj, D. B.; Biju, S.; Reddy, M. L. P. J. Mater. Chem. 2009, 19, 7976 – 7983. (h) Divya, V.; Biju, S.; Luxmi Varma, R.; Reddy, M. L. P. J. Mater. Chem. 2010, 20, 5220 – 5227. (i) Biju, S.; Reddy, M. L. P.;Cowley, A. H.; Vasudevan, K. V. J. Mater. Chem. 2009, 19, 5179 – 5187.
4 (a) V. Divya, S. Biju, R. L. Varma and M. Reddy, J. Mater. Chem., 2010, 20, 5220; (b) L. Fu, R. A. S. Ferreira, N. J. O. Silva, A. J. Fernandes, P. Ribeiro-Claro, I. S. Goncalves, V. d. Z. Bermudez and L. D. Carlos, J. Mater. Chem., 2005, 15, 3117; (c) A. Bellusci, G. Barberio, A. Crispini, M. Ghedini, M. La Deda and D. Pucci, Inorg. Chem., 2005, 44, 1818; (d) D. Li, X. Tian, G. Hu, Q. Zhang, P. Wang, P. Sun, H. Zhou, X. Meng, J. Yang, J. Wu, B. Jin, S. Zhang, X. Tao and Y. Tian, Inorg. Chem., 2011, 50, 7997.
5 Z. M. Hudson, C. Sun, M. G. Helander, Y.-L. Chang, Z.-H. Lu and S. Wang, J. Am. Chem. Soc., 2012, 134, 13930.
6 (a) O. Kotova, R. Daly, C. M. G. dos Santos, M. Boese, P. E. Kruger, J. J. Boland and T. Gunnlaugsson, Angew. Chem., Int. Ed., 2012, 51, 7208 – 7212; (b) W. S. Lo, W. M. Kwok, G. L. Law, C. T. Yeung, C. T. L. Chan, H. L. Yeung, H. K. Kong, C. H. Chen, M. B. Murphy, K. L. Wong and W. T. Wong, Inorg. Chem., 2011,

50, 5309 –5311; (c) R. Shunmugam and G. N. Tew, J. Am. Chem. Soc., 2005, 127, 13567 – 13572; (d) B. Song, G. L. Wang, M. Q. Tan and J. L. Yuan, J. Am. Chem. Soc., 2006, 128, 13442 – 13450; (e) J. Costa, R. Ruloff, L. Burai, L. Helm and A. E. Merbach, J. Am. Chem. Soc., 2005, 127, 5147 – 5157; (f) N. Chandrasekhar and R. Chandrasekar, J. Org. Chem., 2010, 75, 4852 – 4855; (g) C.L. Yang,J. Xu, Y.F. Zhang, Y.W. Li, J. Zheng, L.Y. Liang and M.G Lu. J. Mater. Chem. C, 2013, 1, 4885–4901.

7 A. V. M. Andrade, N. B. Costa, A. M. Simas and G. F. de Sa´, Chem. Phys. Lett., 1994, 227, 349.

8 J. J. P. Stewart, MOPAC 2012 Manual, Stewart Computational Chemistry, Colorado Springs, 2012.

9 (a) A. P. Souza, F. A. A. Paz, R. O. Freire, L. D. Carlos, O. L. Malta, S. A. Junior and G. F. de Sa, J. Phys. Chem. B, 2007, 111, 9228 – 9238; (b) O. Freire, G. B. Rocha and A. M. Simas, Inorg. Chem., 2005, 44, 3299 – 3310.

10 (a) J. Feng and H. Zhang, Chem. Soc. Rev., 2013, 42, 387; (b) Z. L. Xie, H. B. Xu, A. Geßner, M. U. Kumke, M. Priebe, K. M. Fromm and A. Taubert, J. Mater. Chem., 2012, 22, 8110.

11 (a) T. H. Tran, M. M. Lezhnina and U. Kynast, J. Mater. Chem., 2011, 21, 12819; (b) X.-Y. Chen, X. Yang and B. J. Holliday, J. Am. Chem. Soc., 2008, 130, 1546.

12 L. D. Carlos, R. A. S. Ferreira, V. de Zea Bermudez, B. Julián-López and P. Escribano, Chem. Soc. Rev., 2011, 40, 536.

13 (a) J. Phys. Chem. C 2011, 115, 2332-2340; (b) Solar Energy 2011, 85, 2179-2184.

14 (a) P. Myllymaki, M. Roeckerath, J. M. Lopes, J. Schubert, K. Mizohata, M. Putkonen and L. Niinisto, J. Mater. Chem., 2010, 20, 4207; (b) C. Peng, H. Zhang, J. Yu, Q. Meng, L. Fu, H. Li, L. Sun and X. Guo, J. Phys. Chem. B, 2005, 109, 15278; (c) Q. Li and B. Yan, Dalton Trans., 2012, 41, 8567.

15 L. Matthews and E. T. Knobbe, Chem. Mater., 1993, 5, 1697–1700.

16 J. J. P. Stewart, MOPAC 2012 Manual, Stewart Computational Chemistry, Colorado Springs, 2012.

17 (a) X. L. Li,F. R. Dai, L. Y. Zhang, Y. M. Zhu, Q. Peng and Z. N. Chen, Organometallics, 2007, 26, 4483–4490; (b) D. P. Li, C. H. Li, J. Wang, L. C. Kang, T. Wu, Y. Z. Li andX. Z. You, Eur. J. Inorg. Chem., 2009, 4844–4849.

18 D. B. Ambili Raj, Biju Francis, M. L. P. Reddy, Rachel R. Butorac, Vincent M. Lynch, and Alan H. Cowley. Inorg. Chem. 2010, 49, 9055–9063.

19 (a) Jiang Kai, Duclerc Fernandes Parra and Hermi Felinto Brito. J. Mater. Chem., 2008, 18, 4549–4554; (b) D. F. Parra, A. Mucciolo, H. F. Brito and L. C. Thompson, J. Solid State Chem., 2003, 171, 412–419.

20 Y. Hasegawa, Y. Wada, S. Yanagida. J Photochem Photobiol C 2004, 5, 183-202.

21 (a) Silvanose Biju, Ricardo O. Freire, Yu Kyung Eom, Rosario Scopelliti, Jean-Claude G. Bünzli, and Hwan Kyu Kim .Inorg. Chem. 2014, 53, 8407−8417; (b) Alex S. Borges, JoséDiogo L. Dutra, Ricardo O. Freire, Renaldo T. Moura, Jr., Jeferson G. Da Silva, Oscar L. Malta, Maria Helena Araujo, and Hermi F. Brito. Inorg. Chem. 2012, 51, 12867−12878; (c) D. B. Ambili Raj, Biju Francis, M. L. P. Reddy, Rachel R. Butorac, Vincent M. Lynch, and Alan H. Cowley. Inorg. Chem. 2010, 49, 9055-9063.

22 A. Beeby, I.M. Clarkson, R.S. Dickins, S. Faulkner, D. Parker, L. Royle, A.S. Sousa, J.A.G. Williams and M. Woods. *J. Chem. Soc. Perkin. Trans.2.* 1999, 493-504.

23 G.M. Davies, R.J. Aarons, G.R. Motson, J.C. Jeffery, H. Adams, S. Faulkner and M.D. Ward. *Dalton. Trans.* 2004, 1136-1144.

24 A. Balamurugan, M.L.P. Reddy and M. Jayakanna. *J. Phys. Chem. B* 2009, 113, 14128-14138.

25 (a) J.-C. G. B¨unzli and C. Piguet, Chem. Soc. Rev., 2005, 34, 1048–1077; (b) M. H. V. Werts, R. T. F. Jukes and J. W. Verhoeven, Phys. Chem. Chem. Phys., 2002, 4, 1542–1548.

26 (a) Divya, V.; Freire, R. O.; Reddy, M. L. P. Dalton Trans. 2011, 40, 3257−3268; (b) Görller-Walrand, C.; Fluyt, L.; Ceulemans, A.; Carnall, W. T. J.Chem. Phys. 1991, 95, 3099−3106.

27 (a) Boyer, J. C.; Johnson, N. J. J.; van Veggel, F. C. J. M. Chem. Mater. 2009, 21, 2010–2012; (b) Kai, J.; Parrab, D. F.; Brito, H. F. J. Mater. Chem. 2008, 18, 4549–4554; (c) Zhang, H.; Song, H.; Dong, B.; Han, L.; Pan, G.; Bai, X.; Fan, L.; Lu, S.; Zhao, H.; Wang, F. J. Phys. Chem. C 2008, 112, 9155–9162.

28 Foster, T. Ann. Phys. 1948, 2(1-2), 55–75.

The first example of doped Eu-complex/polymer fluorescent films based on PVB as the matrix has been reported.